

and raises the possibility that these proteins might physically interact.

Eukaryotic Ku recruits DNA ligase IV/XRCC4 to sites of DNA damage (8–10). Therefore, we looked for potential interactions between Mt-Ku and Mt-Lig by EMSAs with a radiolabeled dsDNA probe (33 bp). As shown in Fig. 4D, including Mt-Lig and Ku together led to the generation of a DNA-protein complex with a mobility distinct from that of the complexes formed by either protein alone. However, the addition of increasing amounts of Mt-Ku did not abolish the appearance of the novel DNA-protein complex, which strongly suggests that it does not inhibit the binding of Mt-Lig to DNA. Formation of the new complex did not occur if Mt-Lig had been heat denatured (19), which indicates that it reflects the binding of Mt-Lig and is not mediated by a buffer component (Fig. 4D). Biacore studies with a biotinylated dsDNA (33-mer) bound to a streptavidin-coated chip and isothermal titration calorimetry studies also confirmed that Mt-Ku specifically recruits Mt-Lig to DNA (19).

Despite the importance of XRCC4 in the eukaryotic NHEJ system, we have so far been unable to detect any XRCC4 homologs in bacteria (19). It has been reported that many of the Ku-associated DNA ligases possess additional domains with significant homology to eukaryotic DNA primases and nucleases (15, 16). Therefore, it is possible that these domains enhance ligase activity in the absence of XRCC4 and may also be directly involved in the DSB repair process (16). The similarity between the eukaryotic and bacterial Ku proteins suggests that they have evolved from a common ancestor and shows that NHEJ is a much more ancient process than was previously believed. The eukaryotic Ku proteins may have acquired additional domains—such as the VWA, SAP, and DNA-PKcs interaction domains—to enhance the repair activities of the complex and to provide additional functions, such as roles in telomere maintenance and V(D)J recombination. It is notable that only one characterized archaeal species, *Archaeoglobus fulgidus*, contains the Ku ligase system, which suggests that this was acquired by lateral transfer. The Mu phage protein, Gam, and related bacterial orthologs may also represent a distinct family of functional homologs of eukaryotic Ku (30). It is also interesting to note that many of the bacteria that contain the Ku ligase system are capable of sporulation (*B. subtilis*, *S. coelicolor*) and/or spend long periods of their life cycle in the stationary phase (*M. tuberculosis*, *Mesorhizobium loti*, *Sinorhizobium loti*). It is tempting to speculate that a Ku-based NHEJ system is particularly important for the repair of DSBs that arise during these states of relative inactivity, where the better characterized homologous recombination-based repair pathways may be less effective.

References and Notes

1. S. E. Critchlow, S. P. Jackson, *Trends Biochem. Sci.* **23**, 394 (1998).
2. A. Shinohara, T. Ogawa, *Trends Biochem. Sci.* **20**, 387 (1995).
3. W. S. Dynan, S. Yoo, *Nucleic Acids Res.* **26**, 1551 (1998).
4. C. Featherstone, S. P. Jackson, *Mutat. Res.* **434**, 3 (1999).
5. D. Gell, S. P. Jackson, *Nucleic Acids Res.* **17**, 3494 (1999).
6. J. R. Walker, R. A. Corpina, J. Goldberg, *Nature* **412**, 607 (2001).
7. A. J. Doherty, S. P. Jackson, *Curr. Biol.* **11**, R920 (2001).
8. S. A. Nick McElhinny, C. M. Snowden, J. McCarville, D. A. Ramsden, *Mol. Cell. Biol.* **20**, 2996 (2000).
9. L. Chen, K. Trujillo, P. Sung, A. E. Tomkinson, *J. Biol. Chem.* **275**, 26196 (2000).
10. S. H. Teo, S. P. Jackson, *Curr. Biol.* **10**, 165 (2000).
11. A. Dvir, S. R. Peterson, M. W. Knuth, H. Lu, W. S. Dynan, *Proc. Natl. Acad. Sci. U.S.A.* **89**, 11920 (1992).
12. T. M. Gottlieb, S. P. Jackson, *Cell* **72**, 131 (1993).
13. G. C. Smith, S. P. Jackson, *Genes Dev.* **13**, 916 (1999).
14. A. J. Doherty, S. P. Jackson, G. R. Weller, *FEBS Lett.* **500**, 186 (2001).
15. L. Aravind, E. V. Koonin, *Genome Res.* **11**, 1365 (2001).
16. G. R. Weller, A. J. Doherty, *FEBS Lett.* **505**, 340 (2001).
17. T. Dandekar, B. Snel, M. Huynen, P. Bork, *Trends Biochem. Sci.* **23**, 324 (1998).
18. Materials and methods are available as supporting material on Science Online.
19. G. R. Weller *et al.*, unpublished data.
20. M. A. Petit, S. D. Ehrlich, *Nucleic Acids Res.* **28**, 4642 (2000).
21. T. M. Bliss, D. P. Lane, *J. Biol. Chem.* **272**, 5765 (1997).
22. Single-letter abbreviations for the amino acid residues are as follows: A, Ala; C, Cys; D, Asp; E, Glu; F, Phe; G,

- Gly; H, His; I, Ile; K, Lys; L, Leu; M, Met; N, Asn; P, Pro; Q, Gln; R, Arg; S, Ser; T, Thr; V, Val; W, Trp; and Y, Tyr.
23. A. J. Doherty, S. W. Suh, *Nucleic Acids Res.* **28**, 4051 (2000).
24. K. Kodama, D. E. Barnes, T. Lindahl, *Nucleic Acids Res.* **19**, 6093 (1991).
25. V. Sriskanda, S. Shuman, *Nucleic Acids Res.* **26**, 4618 (1998).
26. P. Pfeiffer, S. Thode, J. Hancke, W. Vielmetter, *Mol. Cell. Biol.* **14**, 888 (1994).
27. D. Pang, S. Yoo, W. S. Dynan, M. Jung, A. Dritschilo, *Cancer Res.* **57**, 1412 (1997).
28. R. B. Cary *et al.*, *Proc. Natl. Acad. Sci. U.S.A.* **94**, 4267 (1997).
29. D. A. Ramsden, M. Gellert, *EMBO J.* **17**, 609 (1998).
30. F. d'Adda di Fagnana, G. R. Weller, A. J. Doherty, S. P. Jackson, unpublished data.
31. We thank J. Bradbury for comments on the manuscript, L. Serpell for assistance with figures, T. Kieser for providing *M. tuberculosis* DNA, and P. J. Piggett for supplying *B. subtilis* strains. G.R.W. was supported by a UK Medical Research Council (MRC) studentship. A.J.D. is a Royal Society University Research Fellow, and work in the A.J.D. laboratory is supported by grants from the UK Biotechnology and Biological Sciences Research Council, Cancer Research UK Leukaemia Research Fund, the Association for International Cancer Research, and the Royal Society. Research in the S.P.J. laboratory is supported by grants from Cancer Research UK. B.K. is funded by an MRC grant to P.A.J. R.R. is recipient of a Cambridge Commonwealth Trust Scholarship.

Supporting Online Material

www.sciencemag.org/cgi/content/full/297/5587/1686/DC1
 Materials and Methods
 SOM Text
 Figs. S1 to S6

31 May 2002; accepted 19 July 2002

Mast Cells: A Cellular Link Between Autoantibodies and Inflammatory Arthritis

David M. Lee,^{1,3} Daniel S. Friend,² Michael F. Gurish,^{1,3} Christophe Benoist,^{1,4} Diane Mathis,^{1,4} Michael B. Brenner^{1,3*}

Previous studies have revealed that autoantibodies, complement components, and Fc receptors each participate in the pathogenesis of erosive arthritis in K/BxN mice. However, it is not known which cellular populations are responsive to these inflammatory signals. We find that two strains of mice deficient in mast cells, W/W^y and Sl/Sl^d, were resistant to development of joint inflammation and that susceptibility was restored in the W/W^y strain by mast cell engraftment. Thus, mast cells may function as a cellular link between autoantibodies, soluble mediators, and other effector populations in inflammatory arthritis.

The pathogenic mechanisms at play in inflammatory arthritis, such as rheumatoid arthritis, remain poorly understood both systemically

and in the microenvironment of the diarthrodial joint. A large number of soluble inflammatory mediators and cellular effector populations have been implicated in arthritis; however, the early clinical events remain elusive. Recent studies using the serum of an engineered mouse model, K/BxN, have revealed that autoantibodies directed against a ubiquitously expressed antigen can selectively provoke inflammatory, hyperplastic, and erosive synovitis (1–3). It is known that members of the complement network (the alternative pathway and C5a), Fc receptors (FcγRIII), and cytokines [interleukin

¹Department of Medicine and ²Department of Pathology, Brigham and Women's Hospital, Harvard Medical School, Boston, MA 02115, USA. ³Division of Rheumatology, Immunology and Allergy, Brigham and Women's Hospital; Harvard Medical School, Boston, MA 02115, USA. ⁴Section on Immunology and Immunogenetics, Joslin Diabetes Center, Harvard Medical School, One Joslin Place, Boston, MA 02215, USA.

*To whom correspondence should be addressed. E-mail: mbrenner@rics.bwh.harvard.edu

REPORTS

1 (IL-1), tumor necrosis factor α (TNF- α), as well as neutrophils, have essential roles (4–6). Yet, the pathways leading to the development of synovial pathology by means of these autoantibodies remain to be explained. Given their resident nature in the synovium and their functional capabilities, we hypothesized that mast cells might provide a critical cellular link between soluble factors (autoantibodies and complement, cytokines) and the synovial eruption.

We utilized two strains of mice deficient in mast cells: WCB6F₁ *Kit^{Sl/Sl}Kit^{Sl-d}* (SI/Sl^d) and

WBB6F₁-*Kit^WKit^{W-v}* (W/W^v) (7, 8) to examine the functional role for mast cells in the effector phase of inflammatory arthritis. The SI/Sl^d strain lacks the transmembrane form of stem cell factor (SCF), which results in a deficiency of tissue-resident mast cells (9, 10). After K/BxN serum transfer, control littermates exhibited typical clinical arthritis with synovial hyperplasia, pannus formation, and inflammatory infiltrates (Fig. 1, A, B, and F; and fig. S4A). In contrast, SI/Sl^d mice demonstrated almost no evidence of clinical joint inflam-

mation (Fig. 1, A and B, and fig. S4A) or histopathologic abnormalities (Fig. 1E). Correspondingly, mast cells, many displaying features of degranulation, were identified in inflamed control synovial tissues but not in joint tissues from SI/Sl^d mice (11).

The W/W^v mouse strain also lacks significant numbers of tissue mast cells because of mutations in the SCF receptor, c-kit (12, 13). Similar to findings in the SI/Sl^d strain, W/W^v mice displayed little or no clinical or histologic evidence of arthritis compared with control lit-

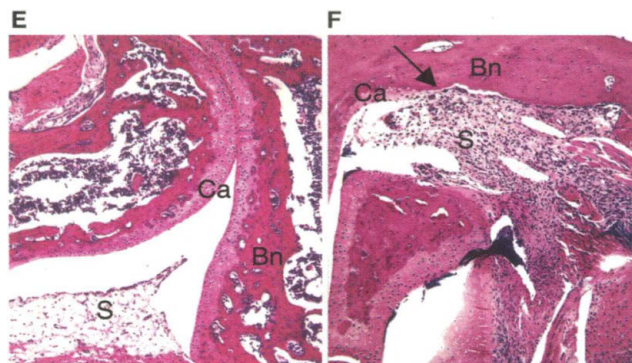
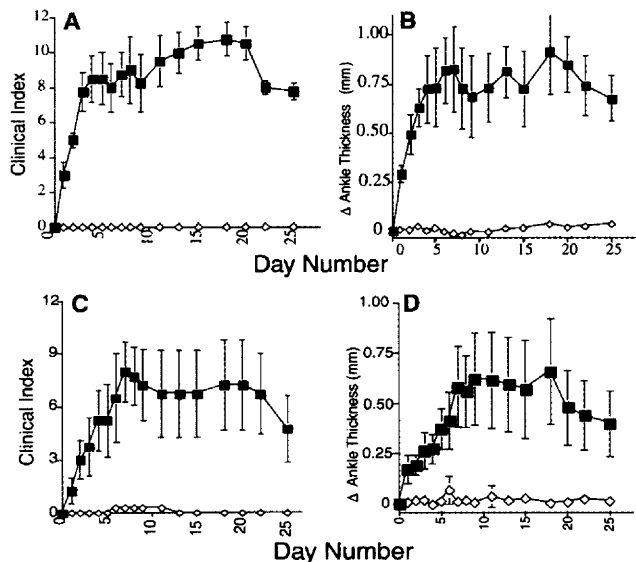


Fig. 1. Attenuation of arthritis in mast cell-deficient SI/Sl^d and W/W^v mice. Arthritogenic K/BxN serum was transferred into 4- to 6-week-old male SI/Sl^d or W/W^v mice and control wild-type littermates as described (3). Clinical index and change in ankle thickness were recorded. (A and B) Wild type (black squares; mean clinical index = 9.5), SI/Sl^d (white diamonds; mean clinical index = 0). (C and D) Wild type (black squares; mean clinical index = 7), W/W^v (white diamonds; mean clinical index = 0). Error bars, SEM. Clinical index (per paw): 0 =

no evidence of inflammation; 1 = subtle inflammation (metatarsal phalanges joints, individual phalanx, or localized edema); 2 = easily identified swelling but localized to either dorsal or ventral surface of paw; and 3 = swelling on all aspects of paw. Maximum score = 12. (E and F) Ankle sections from SI/Sl^d (E) and wild-type (F) mice 11 days after K/BxN serum transfer. SI/Sl^d mice (E) demonstrate thin synovial lining with loose connective tissue in sublining (S), smooth cartilage (Ca), and intact bone (Bn). In contrast, wild-type mice (F) demonstrate synovial lining hyperplasia (S) with inflammatory cellular infiltrates and synovial erosion through cartilage (Ca) into bone (Bn) (arrow). Magnification, $\times 100$. Results are representative of two independent experiments, $n = 3$ or 4 mice per group.

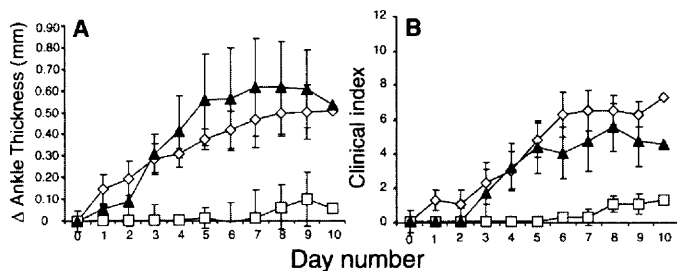
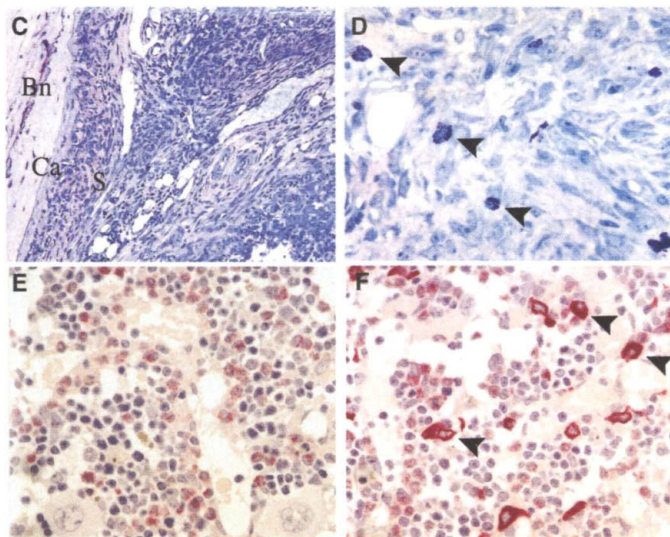


Fig. 2. Restoration of arthritis in mast cell-engrafted W/W^v mice. Selective mast cell engraftment into 20-week-old W/W^v mice was performed by i.v. injection of 1×10^7 cultured BMMCs from wild-type WBB6 F₁ littermates or C57BL/6J donors. BMMCs were derived in 4-week cultures as described (15), with the cytokine concentration modified as follows: 10 ng/ml recombinant IL-3 (rIL-3) and 12.5 ng/ml SCF. DMEM medium was injected as a sham treatment. After allowing 10 weeks for engraftment, arthritogenic K/BxN serum was transferred into sham-injected or BMMC-engrafted W/W^v and control wild-type littermates. Clinical index and change in ankle thickness were recorded. (A and B) Wild type (white diamonds; mean clinical index = 8.4), sham-engrafted W/W^v (white squares; mean clinical index = 0.8), BMMC-engrafted W/W^v (black triangles; mean clinical index = 7). Error bars, SEM. Note: One sham-injected mouse in each experiment developed arthritis. (C) Ankle sections from engrafted W/W^v mice, stained with toluidine blue, reveal synovial (S) hyperplasia and destruction of cartilage (Ca) overlying bone (Bn) 10 days after K/BxN serum transfer. Magnification, $\times 100$. (D) High-power ($\times 500$) view of toluidine blue-stained engrafted synovium demonstrating engrafted mast cells (arrowheads). Separately, mast cell bone marrow engraftment is documented by chloroacetate esterase stain (arrowheads) in BMMC-engrafted (F) but not in sham-injected (E) W/W^v mice. Magnification, $\times 500$. Results are representative of two independent experiments. $n = 4$ to 6 mice per group.



REPORTS

termate mice when exposed to arthritogenic serum from K/BxN mice (Fig. 1, C and D; fig. S1, A and B; and fig. S4B).

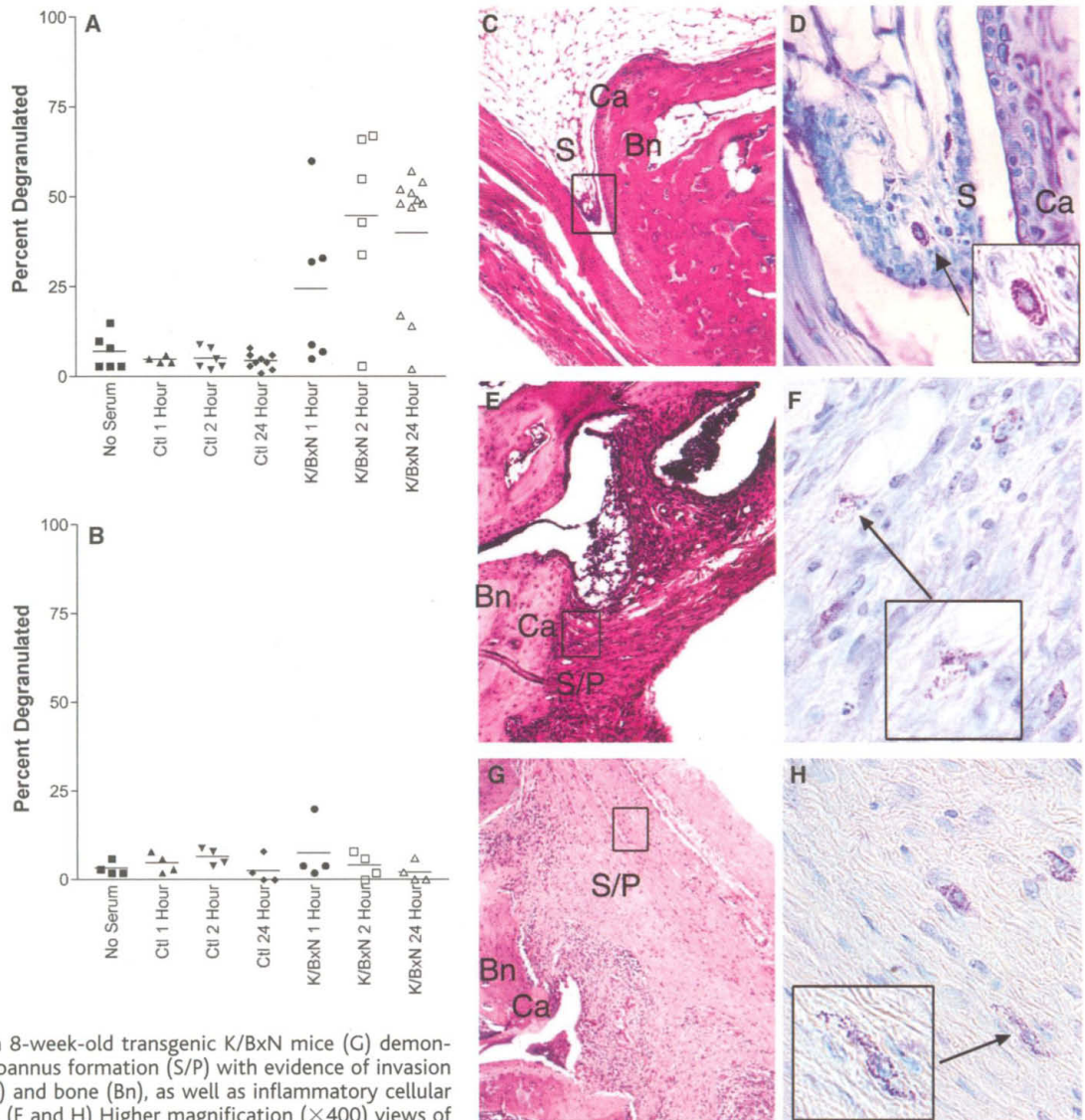
To confirm that the resistance to arthritis after transfer of autoantibody-containing serum was due to the absence of mast cells in the mutant mice, and not to defects in other cellular systems, we performed complementation analysis by assessing the ability of selective mast cell engraftment to confer arthritis susceptibility on these mice. Transfer of either whole bone marrow capable of forming mast cells or bone marrow mast cells (BMMCs) cultured *in vitro* allows selective engraftment of functional tissue-resident mast cells (7, 8, 14). Thus, we cultured wild-type bone marrow cells in IL-3 and SCF for 4 weeks (15) and confirmed expression of FcεR and c-Kit and other histochemical properties of mast cells [fig. S2 and (11)]. These donor BMMCs from wild-type littermates or C57BL/6J mice were then trans-

ferred into W/W^v recipient mice, and engraftment was confirmed 10 weeks later (compare Fig. 2E and 2F). Analysis of a separate series of engrafted W/W^v mice after 22 weeks revealed no correction of anemia, which suggests that this engraftment protocol did not extend to all hematopoietic lineages [fig. S3 and (11)]. The K/BxN serum induced arthritis in these BMMC-engrafted W/W^v mice, whereas most sham-engrafted W/W^v mice remained free of signs of arthritis (Fig. 2, A and B). Similar to wild-type animals, BMMC-engrafted W/W^v mice had degranulated mast cells after K/BxN serum transfer. It is noteworthy that BMMC-engrafted W/W^v mice revealed synovial hyperplasia, cartilage and bone destruction, and inflammatory infiltrates, with neutrophil predominance similar to that typical of control littermates (Fig. 2, C and D; and fig. S4C). In contrast, most sham-engrafted W/W^v mice displayed normal-appearing ankle tissue with

little evidence of synovitis and no discernible mast cells.

Implicit in the potential function of mast cells as a cellular link between soluble components and subsequent arthritogenic events is their activation and the rapid release of potent granule constituents after serum transfer. Therefore, we used a histologic approach to reveal mast cell degranulation and to delineate its time course of activation. Intact mast cells were easily identified in control mice (Fig. 3, A, C, and D), whereas significant mast cell degranulation was noted as early as 1 hour and even more strikingly at 2 and 24 hours after intraperitoneal transfer of K/BxN serum (Fig. 3A). This degranulation preceded the onset of any clinical evidence of inflammation in these animals. In contrast to synovial tissue, no enhanced degranulation was noted in mast cells at other anatomic locations (Fig. 3B). Because degranulation is the clearest histologic hallmark of mast cell activa-

Fig. 3. Histologic analysis of synovial mast cells in arthritis. (A and B) For kinetic analyses of mast cell degranulation, 4-week-old C57BL/6J male mice were injected intraperitoneally with 200 μl of either normal mouse serum (Ctl) or K/BxN serum, and tissues were harvested at the time points indicated. Consecutive mast cells in ankle sections (A) or gastric mucosa (B) were visually assessed for intact versus degranulating phenotype in a blinded fashion. Shown are results from individual mice pooled from three separate experiments. Horizontal bars represent mean percent degranulation. Ankle tissues from normal (C and D) and arthritic C57BL/6J (E and F) and K/BxN (G and H) mice were fixed and stained with hematoxylin and eosin [(C), (E), and (G)] or toluidine blue [(D), (F), and (H)]. (C) Normal mice demonstrate thin synovial lining and loose connective tissue sublining (S), smooth cartilage (Ca), and intact bone (Bn). Magnification, ×100. (D) View (×400) of tissue outlined in (C) demonstrating intact mast cells, with compact metachromatically staining granules (inset), which are present sparsely throughout the synovium. Ankle sections obtained 12 days after transfer of arthritogenic K/BxN serum (E) and in 8-week-old transgenic K/BxN mice (G) demonstrate synovial hyperplasia and pannus formation (S/P) with evidence of invasion and destruction of cartilage (Ca) and bone (Bn), as well as inflammatory cellular infiltrates. Magnification, ×100. (F and H) Higher magnification (×400) views of toluidine blue-stained tissue outlined in (E) and (G), which demonstrate degranulating and intact mast cells. Insets show high magnification (×1000) of degranulating mast cells.



tion, the presence of degranulated mast cells in joint tissue, and not other tissues, before overt clinical or histologic inflammation supports a proximal, synovium-specific role for mast cells in the effector phase of inflammatory arthritis. Moreover, because mast cells continue to demonstrate a degranulating phenotype during more chronic phases of arthritis (Fig. 3, E to H), it is also likely they play an ongoing role in the arthritic process.

Initial results from the mast cell-deficient mouse strains left open the possibility that the SCF/c-kit signaling pathway played some role in the induction of arthritis other than via mast cells. However, the restoration of arthritis susceptibility by mast cell engraftment defined mast cells as the element that prevents disease development in SI/SI^d and W/W^v mice. The striking requirement for mast cells, coupled with evidence for their rapid degranulation within the first hours after serum transfer, leads us to suggest that mast cells may provide the cellular target of autoantibodies, the complement network, and Fc receptors in the subsequent development of inflammatory arthritis. Because C5a and FcγR ligation are potent activators of mast cell function in vitro and in vivo (16–22), it is likely that synovial mast cells are activated by articular autoantibody immune complexes suggestive of an immune complex hypersensitivity (Arthus) reaction in the synovium (23, 24).

Mast cells themselves produce a series of effector molecules that mediate permeability, inflammation, chemotaxis, and tissue destruction. They are the only cells that contain preformed TNF-α in granules and they also display an ability to rapidly produce large amounts of both TNF-α and IL-1 (25, 26), cytokines that play a critical role in K/BxN arthritis (6), as well as in human rheumatoid arthritis. Mast cell granules also contain an abundance of proteases capable of activating matrix metalloproteinases (27) and mMCP-6, a potent indirect neutrophil chemoattractant (28). These cells also produce large quantities of other inflammatory molecules including histamine, eicosanoids, fibroblast growth factor, and angiogenesis factors (VEGF), which may contribute further to the arthritic process.

Historically, mast cells have been implicated in two contrasting types of immune responses. First, they can be activated by immunoglobulin IgE receptors to mediate immediate hypersensitivity reactions associated with allergic phenomena. Second, their acute activation by microbial products, as in bacterial peritonitis models, underscores their role in infection (29, 30). Here, we present evidence of a direct role for mast cells in the pathogenesis of inflammatory arthritis. Our findings in the K/BxN model of destructive arthritis point to a likely role for mast cells in human arthritis associated with immune complex formation, namely, cryoglobulin-associated synovitis in hepatitis C infection, postinfectious arthritis, and perhaps others. Moreover, histo-

logic analyses of synovial sections from humans have documented the presence of mast cells in abundance (22) and immune complexes, complement fragments, and SCF are present in synovial fluid and tissue in rheumatoid arthritis (31–33). Together, these findings illustrate that mast cells can contribute to the pathogenic mechanisms in the synovium that result in erosive arthritis.

References and Notes

1. I. Matsumoto, A. Staub, C. Benoist, D. Mathis, *Science* **286**, 1732 (1999).
2. V. Kouskoff et al., *Cell* **87**, 811 (1996).
3. A. S. Korganow et al., *Immunity* **10**, 451 (1999).
4. B. T. Wipke, P. M. Allen, *J. Immunol.* **167**, 1601 (2001).
5. H. Ji et al., *Immunity* **16**, 157 (2002).
6. H. Ji et al., *J. Exp. Med.* **196**, 77 (2002).
7. Y. Kitamura, S. Go, K. Hatanaka, *Blood* **52**, 447 (1978).
8. Y. Kitamura et al., *J. Exp. Med.* **150**, 482 (1979).
9. C. I. Brannan et al., *Proc. Natl. Acad. Sci. U.S.A.* **88**, 4671 (1991).
10. K. M. Zsebo et al., *Cell* **63**, 213 (1990).
11. D. M. Lee et al., unpublished observations.
12. K. Nocka et al., *EMBO J.* **9**, 1805 (1990).
13. E. N. Geissler, M. A. Ryan, D. E. Housman, *Cell* **55**, 185 (1988).
14. T. Nakano et al., *J. Exp. Med.* **162**, 1025 (1985).
15. M. F. Gurish et al., *J. Exp. Med.* **175**, 1003 (1992).
16. W. Fureder et al., *J. Immunol.* **155**, 3152 (1995).

17. G. Alber, U. M. Kent, H. Metzger, *J. Immunol.* **149**, 2428 (1992).
18. H. R. Katz et al., *J. Immunol.* **148**, 868 (1992).
19. U. Baumann et al., *J. Immunol.* **164**, 1065 (2000).
20. U. Baumann et al., *J. Immunol.* **167**, 1022 (2001).
21. D. Dombrowicz et al., *J. Clin. Invest.* **99**, 915 (1997).
22. H. P. Kiener et al., *Arthritis Rheum.* **41**, 233 (1998).
23. I. Matsumoto et al., *Nature Immunol.* **3**, 360 (2002).
24. D. L. Sylvestre, J. V. Ravetch, *Immunity* **5**, 387 (1996).
25. J. R. Gordon, S. J. Galli, *Nature* **346**, 274 (1990).
26. P. R. Burd et al., *J. Exp. Med.* **170**, 245 (1989).
27. K. Suzuki, M. Lees, G. F. Newlands, H. Nagase, D. E. Woolley, *Biochem. J.* **305**, 301 (1995).
28. C. Huang et al., *J. Immunol.* **160**, 1910 (1998).
29. B. Echtenacher, D. N. Mannel, L. Hultner, *Nature* **381**, 75 (1996).
30. R. Malaviya, T. Ikeda, E. Ross, S. N. Abraham, *Nature* **381**, 77 (1996).
31. I. Broder, M. B. Urowitz, D. A. Gordon, *Med. Clin. N. Am.* **56**, 529 (1972).
32. V. E. Jones, R. K. Jacoby, P. J. Cowley, C. Warren, *Clin. Exp. Immunol.* **49**, 31 (1982).
33. M. Schaller, D. R. Burton, H. J. Ditzel, *Nature Immunol.* **2**, 746 (2001).
34. The authors gratefully acknowledge the insightful discussions and manuscript review by K. F. Austen, as well as the expert technical assistance of the histotechnicians A. Calderone, T. Bowman, D. Bowman, and L. Chen. This work was supported by NIH grant 1R01 AR/Al46580-01 (to D.M. and C.B.).

Supporting Online Material

www.sciencemag.org/cgi/content/full/297/5587/1689/DC1

Materials and Methods
Figs. S1 to S4

8 May 2002; accepted 25 July 2002

Structure, Mechanism, and Regulation of the *Neurospora* Plasma Membrane H⁺-ATPase

Werner Kühlbrandt, Johan Zeelen, Jens Dietrich*

Proton pumps in the plasma membrane of plants and yeasts maintain the intracellular pH and membrane potential. To gain insight into the molecular mechanisms of proton pumping, we built an atomic homology model of the proton pump based on the 2.6 angstrom x-ray structure of the related Ca²⁺ pump from rabbit sarcoplasmic reticulum. The model, when fitted to an 8 angstrom map of the *Neurospora* proton pump determined by electron microscopy, reveals the likely path of the proton through the membrane and shows that the nucleotide-binding domain rotates by ~70° to deliver adenosine triphosphate (ATP) to the phosphorylation site. A synthetic peptide corresponding to the carboxyl-terminal regulatory domain stimulates ATPase activity, suggesting a mechanism for proton transport regulation.

P-type ATPases are ion pumps of ~100 kD that use ATP to transport cations through the cell membrane against a concentration gradient (1). The proton ATPases in the plasma membrane of fungal and plant cells maintain the intracellular pH and membrane potential, providing energy for the uptake of nutrients and exchange of ions by

secondary transporters. The pumps cycle between the E1 and E2 states, which have different binding affinities for nucleotides and for the transported ion. A conserved aspartate (Asp³⁷⁸ in the *Neurospora* proton ATPase) is reversibly phosphorylated (1) after the proton binds to a site in the membrane from the cytoplasmic side. Phosphorylation of the aspartate results in a conformational change. This reduces affinity of the binding site for the proton that is released to the outside. Large conformational changes occurring during the pumping cycle (2, 3) were apparent from a comparison

Max-Planck-Institut für Biophysik, Heinrich-Hoffmann-Str. 7, 60528 Frankfurt am Main, Germany.

*Present address: Laboratory of Molecular Biophysics, University of Oxford, South Parks Road, Oxford OX1 3QU, UK.